RESEARCH PAPER

NaOH/Microwave-Assisted Synthesis of Carbonate-Rich Activated Charcoal for Catalytic Oxidation of Nitrite in Aqueous Solution

Sumrit Mopoung*, Rinlaphat Thanakulwaranon

* *sumritm@nu.ac.th*

Chemistry department, Faculty of Science, Naresuan University, Thailand

Received: November 2025 **Revised: February 2026** **Accepted: May 2026**
DOI: 10.22068/ijmse.4430

Abstract: *Activated charcoals were prepared by activation with 600 W microwave irradiation in combination with pretreatments of tamarind wood derived charcoal in boiling mixtures with NaOH (1 g: 0 g-1 g: 0.12 g). The samples were characterized by FTIR, XRD, SEM-EDS, and BET, and used for catalytic nitrite oxidation under an air atmosphere in the absence of light at 30°C, pH 6.5, and 120 rpm shaking for improved efficiency. The results show that the percent yields of tamarind wood-derived activated charcoals (ACCs) were 88.51%-94.66%. The main carbonate compounds of ACCs are present in the materials after activation. Na^+ ions and water molecules could be inserted into the graphitic layers during pretreatment and efficiently effected surface cracking of ACCs by 600 W microwave irradiation. The surface cracklings and porosities of ACCs increased with increasing NaOH concentration from 1 M to 3 M, with an optimum at 2 M NaOH. The final products are mesoporous materials containing macro- and meso-hole channels. It was found that the nitrite conversions exhibit high reaction rates within 20 min. The reactions proceed via catalytic oxidations, and their rates increase with increasing concentrations of NaOH activation, while nitrite conversions via the disproportionation reaction were inhibited. The optimized catalyst with 1 g: 0.08 g activation ratio enhanced the oxidation conversion by up to 36% compared to the catalyst-free system. In addition, spent ACCs with 1 g: 0.04 g-1 g: 0.12 g activation ratios remained stable and exhibited catalytic oxidation activity after three catalytic cycles, with oxidation conversion efficiency consistently falling in the range of 32.22%-49.48%.*

Keywords: *Microwave irradiation, Sodium hydroxide, Activated charcoal, Catalytic oxidation, Nitrite.*

1. INTRODUCTION

Nitrite is usually found in aquatic environments and originates from fertilizer use, manure applications, and sewage discharge. It is a human carcinogen and can cause methemoglobinemia [1]. Therefore, it is necessary to eliminate nitrite present in wastewater. The most widely used methods used in the past were catalytic reduction, γ-ray irradiation, and ion exchange, but these are expensive, relatively slow, and complex [2, 3]. Nitrite can be both reduced and oxidized via a disproportionation reaction, which transforms it from its oxidation state of +3 to the oxidation state of +2 in nitric oxide and the oxidation state of +5 in nitrate, under ambient conditions in natural environments [1]. On the other hand, the nitrite oxidation reaction, which involves the addition of an oxygen atom to the nitrite ion and produces only the nitrate ion, is also possible. However, there is very little research reported for the nitrite oxidation reaction, especially catalytic oxidation. Normally, the competitive relationship between oxidation and disproportionation reaction pathways in the liquid phase ultimately suppresses NO_2^- oxidation efficiency [2]. The disproportionation is an undesirable side reaction, which releases NO gas, causing secondary pollution, while the oxidation reaction produces only nitrate ions, which are more stable and cause less pollution [4]. Therefore, the use of the oxidation reaction for nitrite conversion to nitrate is desirable for environmental water treatment. Nitrite oxidation reactions include the nitrification process by nitrite oxidoreductases from nitrite-oxidizing bacteria, chemical oxidation by an oxidizing agent [eg. CeO_2, MnO_2], and metal oxide doped catalysts [2, 4]. The photocatalysis by semiconducting materials [5, 6] and electrocatalysts in the form of suspension, immobilized layer on the surface of an electrode, or immobilized on any other inert material [3, 5] is also used for nitrite conversion by catalytic oxidation. However, nitrite is highly soluble in water and has a low affinity for most natural sorbents, and thus it is mobile and persistent in the environment [1]. In addition, achieving nitrite removal via nitrification would be time-consuming [2]. This problem could be solved by adsorbent materials, which could immobilize nitrite for enhanced oxidation reaction via surface catalytic transformation. Catalytic oxidation on

[DOI: 10.22068/ijmse.4430]

the surface of a catalytic adsorber involves oxygen molecules from the air reacting with nitrite ions on the surface of the catalysts to form nitrate [7]. On the other hand, the disproportionation reaction involves the nitrite ions transforming internally into both nitrate and a lower oxidation state nitrogen compound [1]. However, the disproportionation reaction could be inhibited by pH >5 [8], anionic surfactants (sodium dodecyl benzene sulfonate and sodium dodecyl sulfonate in aerobic denitrification) [9], metal-oxide electrocatalysts (NiCo oxide composite) [10], and scavenger intermediates (eg. polymerization, free radicals) [11]. On the other hand, some catalysts have been used for nitrite oxidation conversion to nitrate, such as zeolites, metal-exchanged zeolites, carbon materials, metal oxides, and metal-based catalysts [2]. The atmospheric conditions, which have been used for nitrite oxidation, are pure oxygen [8], ozone [2, 12], and air [6]. Hydrogen peroxide has also been used for the oxidation of ammonia to nitrite and subsequently to nitrate [13]. However, there is very little reported research on the nitrite oxidation reaction, especially using carbon-based materials for catalytic oxidation. There are some reports that have described the use of zeolites [8], Mn-zeolites, aluminosilicates [2], and TiO_2 nanoparticle-acrylic [6] for nitrite catalytic oxidation under pH 3-4 with oxygen, oxygen-ozone, ozone, or air atmosphere. Undesired disproportionation reactions were also observed in these reports. Therefore, this research is focused on the preparation of activated charcoal to be used for nitrite conversion into nitrate via surface catalytic oxidation under mild conditions without disproportionation reaction. In general, activated carbons have been produced by physical activation by oxidizing gases like steam, air, and CO_2, and by chemical activation with dehydrating chemical agents, including phosphoric acid, sulfuric acid, potassium hydroxide, and zinc chloride, at high temperatures and under an inert atmosphere [14]. NaOH is an oxidizing chemical agent, which is used for the preparation of activated carbon materials by causing dehydration, oxidation, and reduction reactions that erode the carbon structure and create pores, resulting in high-surface-area materials with excellent adsorption properties [15]. In this research, NaOH was used for chemical activation along with microwave irradiation for the preparation of activated charcoal. It is expected that the final products will have a basic character inhibiting the disproportionation reaction. Moreover, microwave irradiation co-activation may reduce the activation reaction time. It was reported that thermal plasma treatment by microwave power of 800 W for activated carbon preparation could induce a disordered structure along with the decrease of oxygen on the surface within 5 min of irradiation time [16]. Activated carbon products with abundant surface hydroxyl species, which are prepared by microwave irradiation and sodium hydroxide, have been used for desulfurization of coal with high efficiency [17]. This method was also used for the activation of sawdust, which produced mesoporous structured activated carbon that resulted in the demolition of cellulose and hemicelluloses, lignin solubilization, and swelling of biomass samples [18]. In the same way, activated carbon products made from biodiesel industry solid residues are mainly macro and mesoporous materials [19]. It was shown that porous activated carbons made using NaOH along with microwave irradiation depended on the types of raw materials. However, the use of simple, carbonate-containing NaOH/microwave-activated charcoal for the selective catalytic oxidation of nitrite under mild, ambient air conditions has not been reported.

The objective of this research was to study the effects of NaOH concentration and 600 W microwave irradiation power on the activation of tamarind wood charcoal. The physical and chemical characteristics of the final products were investigated by FTIR, FESEM-EDS, and BET analysis. Finally, nitrite catalytic oxidation conversion into final products was investigated under conditions close to the natural environment.

2. EXPERIMENTAL PROCEDURES

2.1. Activated Charcoal Preparation

Tamarind wood-derived charcoal (CC) was prepared using carbonization at around 500°C and was obtained from a local traditional kiln at Bankrang district, Phitsanulok province, Thailand. It was ground and screened by 60 mesh sieves (Laboratory test sieve, Retsch, Germany). The powder CC was dried in an oven (SL 1375 SHEL LAB 1350FX) at 105°C for 3 h. Samples of the dried CC powders (20 g, weighed by Sartorius ED224s, Germany) were impregnated with 0 M–3 M NaOH (reagent grade, Merck, Germany) solution with a ratio of 1:1 of CC weight to NaOH volume (calculated as weight charcoal per weight NaOH= 1 g: 0 g, 1 g:

[DOI: 10.22068/ijmse.4430]

0.04 g, 1 g: 0.08 g and 1 g: 0.12 g). The samples were pretreated by boiling at 100°C for 1 h. After that, the samples were microwave irradiated with 600 watts (SAMSUNG ME711K, 20 L, Bangkok, Thailand) for 15 mins in the absence of inert gas, following the report of Liew et al. [20], to provide no excessive heat energy for pore development. The final product powders were dried at 100°C in an oven for 3 h and weighed. The percent yields of the final products were calculated. The dried CC and dried final products (ACC0-600–ACC3-600) were characterized by FTIR (Spectrum GX, Perkin Elmer, Connecticut, USA), XRD (PW 3040/60, X' Pert Pro Console, Philips, Netherlands), FESEM-EDS (Leo1455VP Electron Microscopy, Cambridge, England), and BET analysis (Micromeritics TriStar II3020, Bavaria, Germany). All products were used as catalysts for the oxidation conversion of nitrite to nitrate in aqueous solution.

2.2. Catalytic Oxidation of Nitrite Experiment

The catalytic oxidation of nitrite to nitrate by CC or ACCs follows Eq. (1) [8]:

$$2NO_2^- (aq) + O_2 (g) \rightarrow 2NO_3^- (aq) \quad (1)$$

However, the disproportionation reaction of NO_2^- under relatively acidic conditions, which is an undesirable side reaction, may also occur (Eq. (2)) [8]:

$$3NO_2^+ (aq) + 2H^+ (aq) = 2NO (g) + NO_3^- (aq) + H_2O (l) \quad (2)$$

Therefore, both catalytic oxidation and dis-proportionation reactions are considered in this experiment.

2.3. The Effect of Dosage

The conversion of nitrite to nitrate by using air as an oxidant under an air atmosphere in the absence of light was carried out in batch experiments with ACC2-600 dosage of 0-8 g/L of ACC2-600 in triplicate. Aqueous 100 mg/L NO_2^- solutions (100 mL) containing 0-0.8 g of ACC2-600 were placed into 250 mL conical flasks. The pH of all aqueous solutions was adjusted to 6.5 by using 0.1 M HCl solution (lab grade, Merck, Germany) and NaOH aqueous solutions (lab grade, Merck, Germany) using a pH meter (Mettler Toledo, Hamilton, New Zealand). Subsequently, all solutions were put in a shaking water bath (ESSSTELL-ESB, South Korea) and then shaken continuously at 120 rpm at a temperature of 30±2°C for 120 min while being open to the air atmosphere in the absence of light. After that, the aqueous phase was separated by centrifuge (Onilap-DM0636, USA) at 4000 rpm for 10 min and filtered through a Whatman No. 42 filter paper. The concentrations of NO_2^- and NO_3^- in all filtrates were measured by the diazotization colorimetric method [21]. This is a spectrophotometric method [22], which uses a UV/Visible spectrometer (UNICO 1100, Georgia, USA) detecting NO_2^- and NO_3^- by measurement of absorbance values at 507 nm, and 220 nm, respectively. The concentrations of the nitrite and nitrate in filtrate solutions were calculated from the absorbance values using a standard calibration curve. The total NO_2^- conversion (NC_T) at 120 min was calculated according to (Eq. (3)):

$$NC_T\% = [(C_{i\ nitrite} - C_{f\ nitrite})/C_{i\ nitrite}] \times 100 \quad (3)$$

Percent of nitrite conversion via disproportionation reaction (NC_D) from NO_2^- lost as NO (Eq. (4)), which was modified from the study of Ying et al. [8]:

$$NC_D\% = \{[(C_{initrite} - C_{fnitrite}) - (C_{fnitrate} - C_{initrate})]/C_{initrite}\} \times 100 \quad (4)$$

Where $C_{initrite}$ and $C_{fnitrite}$ refer to the initial and final NO_2^- concentration, and $C_{initrate}$ and $C_{fnitrate}$ refer to the initial and final NO_3^- concentration, respectively.

Percent of nitrite conversion via oxidation reaction (NC_O) was calculated following (Eq. (5)) modified form report of Ying et al. [8]:

$$NC_O\% = NC_T\% - NC_D\% \quad (5)$$

2.4. The Effect of Reaction Time

Batch experiments were also used to investigate the effect of reaction time (0-120 minutes) to determine the time needed for maximum conversion. The aqueous solutions (100 mL of 100 mg/L NO_2^-) containing 0 g or 0.3 g (3 g/L) of ACC2-600 were placed into 250 mL conical flasks and put in the water bath to maintain the temperature of 30±2°C. All experiments were operated in the same way as the experiments used to determine the effect of dosage. Aqueous solution samples were drawn every 15 min and were filtered through a Whatman No. 42 filter paper. The concentrations of NO_2^- and NO_3^- of all filtrates were measured and calculated. The percent of NC_T was calculated using Eq (3).

2.5. The Effects of NaOH Concentration, Activation and Recycling

All experiments were operated in the same way as the time effect experiments with or without 3 g/L of CC or ACC0-600–ACC3-600 for 60 min. The

[DOI: 10.22068/ijmse.4430]

percentage values of NC_T, NC_D, and NC_O were calculated using Eqs. (3-5). In addition, all remaining catalyst solids obtained after filtration were dried at 50°C in a vacuum oven (VO500, Memmert, Germany) and weighed (BSA, Sartorius, Germany). All solids were used for catalyst recycling in two subsequent repeats of the reaction. The amount of recovered catalyst used in the repeat reactions was 0.21 g for the first recycling round and 0.15 g for the second recycling round. Solutions of 100 mg/L NO_2^-, 50 mL, and 70 mL were used to maintain a constant dosage concentration of 3 g CC or ACCs/L for the first recycling and the second recycling experiments, respectively. All catalyst residues from all reaction repeats were dried and weighed. The percentage of loss values of dried weights of the catalysts in each reaction repeat was calculated and compared. The ACC2-600 residue obtained after all repeat reactions was characterized by FTIR for comparison with fresh ACC2-600.

3. RESULTS AND DISCUSSION

3.1. Percent Yields of Charcoal and Activated Charcoals

Main chemical reactions during NaOH activation have been proposed in the following equations (Eqs. (6) to (10)) [23]:

$$2NaOH\ (aq) \rightarrow Na_2O\ (s) + H_2O\ (l) \quad (6)$$

$$CO_2\ (g) + Na_2O\ (s) \rightarrow Na_2CO_3\ (s) \quad (7)$$

$$Na_2CO_3\ (s) \rightarrow Na_2O\ (s) + CO_2\ (g) \quad (8)$$

$$Na_2O\ (s) + 2C\ (s) \rightarrow Na\ (s) + 2CO\ (g) \quad (9)$$

$$Na_2CO_3\ (s) + C\ (s) \rightarrow 2Na\ (s) + 3CO\ (g) \quad (10)$$

Minor water-gas reaction with water is also occurring during the microwave activation as described in the following Eq. (11) [14];

$$C\ (s) + H_2O\ (g) \rightarrow CO\ (g) + H_2\ (g) \quad (11)$$

Another water-gas shift reaction can take place according to Eq. (12) [24];

$$CO\ (g) + H_2O\ (g) \rightleftharpoons CO_2\ (g) + H_2\ (g) \quad (12)$$

The percent yield of CC made from tamarind wood is quite high (Fig. 1). This is because tamarind wood is a hardwood with low volatile matter content (37.82%) and high fixed carbon content (58.30%) [25]. The volatile matters were released by thermal degradation during the carbonization stage. Percent yields of the ACCs obtained after the activation process are low, with values in the range between 35.65% and 38.13%, when calculated based on tamarind wood weight or between 88.51% and 94.66%, when calculated based on CC weight. For 0 M NaOH and 600 W microwave irradiation, the carbon atoms present in the CC performed as good microwave absorbents with induced dipole rotation of carbon-based molecules at the rate of a million times per second. This process produced a frictional force and released heat for partial oxidation activation [26]. However, the results showed that the percent yield of the partial oxidation (Eqs. (9-10)) of some of the original compounds in raw CC and water is a little reduced. In the case of activation with 1 M–3 M NaOH and 600 W microwave irradiation, the NaOH at various concentrations and some oxygen from air (in the absence of inert gas) resulted in a gradual decrease of the ACCs percent yields along with sodium oxide and carbonate species formation, which was attributed to the microwave irradiation. It was shown that the carbon content in CC decreases minimally during activation under these conditions. However, a trend of increasing losses of carbon can be observed with increasing NaOH concentrations. This is attributed to the energized solvated sodium complex, which contains high heat energy, which could cause highly vigorous motions (e.g., translational motion and rotational motion) on the CC surface.

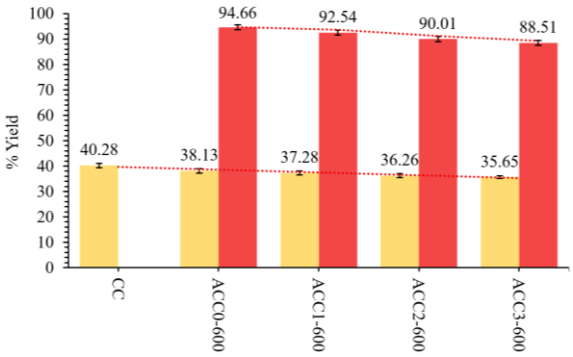

Fig. 1. Percent yields of CC and ACCs with 600 W microwave power and 0-3 M NaOH activation. (A) percent yields were calculated based on raw tamarind wood weights, and (B) percent yields of ACCs were calculated based on charcoal weights (the error bars represent standard deviation).

This indicates that when higher amounts of NaOH were used, more NaOH molecules were available to break the chemical bonds present within the CC matrix, which in turn enhanced the removal of some carbon components in the form of volatiles (e.g., CH_4, CO_2, or CO) during the process of activation by microwave irradiation [20]. Another role of NaOH is minimizing the formation of tars and any other liquids (dehydrating agents) that

[DOI: 10.22068/ijmse.4430]

could possibly clog up the pores and inhibit the partial oxidation necessary for the development of porous structures in the ACCs [26]. This effect allows more NaOH to be exposed to the carbon elements within the CC matrix.

3.2. Elemental Composition of CC and ACCs

Table 1 shows that the main element present on the surface of CC and ACCs from tamarind wood is carbon, with oxygen acting as the secondary element. In addition, small amounts of Ca, Na, and K elements have also appeared within both CC and ACCs. However, the content of these elements increased after activation with 0 M to 3 M NaOH and 600 W microwave irradiation. The oxygen content has a similar tendency, while the carbon content shows an opposite trend. For CC, the carbon content is quite high. This shows that the carbonization of tamarind wood is quite complete with low oxygen content. Moreover, CC also contains Ca, Na, and K, which are components in the raw tamarind wood. These elements acted as catalysts for the cracking of organic tar compounds [27]. The increasing content of Ca, Na, and K elements, which do not undergo thermal degradation, is attributed to the more extensive degradation of carbon content during activation by 0 M to 3 M NaOH. Especially, Na element content increased with increasing NaOH concentration used for pretreatment and activation. The increasing content of oxygen observed with increasing NaOH concentration from 0 M to 3 M is attributed to the increasing extent of partial oxidation by NaOH in its role as an oxidizing agent and due to the reaction with some oxygen from air during activation. While carbon content was more extensively degraded by thermal gasification by water-gas reaction or water-gas shift reaction (Eqs. (11-12)) with increasing NaOH concentrations, which release CO_2, CO, and carboxylic acids [20]. These results confirmed that partial oxidation reactions occurred during the activation process.

Table 1. Elemental composition from EDS of CC and ACCs

Samples	Elements composition (wt.%)				
	C	O	Ca	Na	K
CC	97.2	2.2	0.2	0.1	0.1
ACC0-600	94.1	7.8	0.3	0.1	0.2
ACC1-600	90.7	8.0	0.3	0.8	0.3
ACC2-600	87.5	9.9	0.5	1.6	0.4
ACC3-600	85.7	10.9	0.6	2.3	0.5

3.3. Surface Chemistry of CC and ACCs by FTIR

FTIR transmission spectrum of CC exhibits smooth spectral lines corresponding to OH, C=C, and C-O functional groups (Fig. 2a). These surface functional groups are attributed to the decomposition of lignocellulosic components via dehydration, carbon rearrangement, and breaking of alkyl-aryl linkages to release water, carbon monoxide, and carbon dioxide molecules during the carbonization process [20]. This has confirmed that tamarind wood is essentially completely carbonized, leading to a material with the dominance of aromatic graphitic structure. The OH and CO surface groups formed from adsorbed water and carboxylic acids, which resulted from the gasification reaction and the reaction of CO with OH^- ion during carbonization, respectively [23]. While C=C groups represent more extensive development of aromatic carbon character [23]. After activation with only water and 600 W microwave irradiation (Fig. 2b), some functional groups, such as OH of the free water of the topmost water layer (free water at 3845 cm^{-1}) [28], C=O of the carbonyl [29], and carbonate salts with Na, Ca, and K [30], occurred.

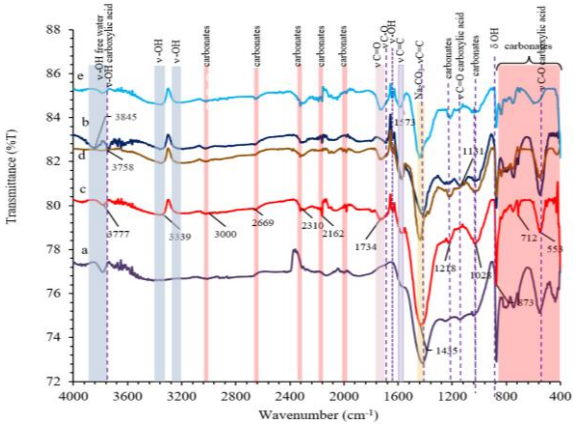

Fig. 2. FTIR transmission spectra of a) CC, b) ACC0-600, c) ACC1-600, d) ACC2-600, and e) ACC3-600

These surface functional groups were formed by thermal microwave irradiation and the catalytic effects of some compounds present in the original CC. A band between about 3800-3900 cm^{-1} can be assigned to the OH group. It corresponds to the stretching mode of free water [28], which penetrated the graphene layers of CC during microwave activation. Furthermore, water-gas reaction, which is based on the reactivity of water vapor in the heterogeneous steam reforming, has

[DOI: 10.22068/ijmse.4430]

also occurred during microwave activation (Eq. (11)) [14] with CO being formed. This CO can also react with OH^- ion to produce the carboxylic (COOH) acid on close-packed surfaces [24], which is demonstrated through a slight increase in intensities of the peaks at about 3758 cm^{-1}, 1131 cm^{-1}, and 553 cm^{-1}. After activation with NaOH and microwave irradiation, these functional groups decrease or disappear with increasing NaOH concentration. Because carboxylic acid groups were weakened by hydroxyl ions during the NaOH pretreatment stage [20], peaks corresponding to the aromatic structure became dominant with increased intensities of C=C at 1573 cm^{-1} and 1435 cm^{-1} [23]. This is because irradiation with 600 W microwave power could produce enough energy to break the single carbon–carbon bonds, inducing the rearrangement reaction of the carbon atoms to form more complex polycyclic structures, while the carbon–carbon double bond in the CC cannot be broken with this level of microwave irradiation [20]. Furthermore, the transmission spectra intensities of carbonated groups, especially those dominated by carbonate in the Na_2CO_3 form, increased with increasing NaOH concentrations from 1 M to 3 M and 600 W microwave irradiation activation (Fig. 2b-e). This result has shown that the more violent activation with NaOH took place, and surface carbon structures are formed (Eqs. (6-10)). At the same time, OH groups of adsorbed water and penetrated water in graphitic layers of ACCs have remained at a stable level due to strong attraction. On the other hand, the intensity of the C=C group gradually decreased. This showed that the aromatic characteristics of ACCs decrease a little with increasing NaOH concentrations from 0 M to 3 M. Finally, the peak corresponding to the C=O group at 1734 cm^{-1} also underwent a relative increase with increasing NaOH concentration. This peak is attributed to carbonyl groups within the carbon structure, which exist with strong intermolecular interaction between sodium ions and oxygen atoms by a coordinate bond in the carbon structure [29].

3.4. Structural Characterization of CC and ACCs by XRD

The XRD patterns of CC and ACCs confirmed the presence of amorphous carbon allotropes and carbonated compounds (Fig. 3a-e), which is consistent with the results of FTIR. All XRD patterns of CC and ACCs exhibit two broad diffractions at 22.4° and 43.5°, which correspond to the disordered and ordered graphite structures, respectively [31]. However, disordered graphitic characteristics increased with activation from 0 M to 3 M NaOH. This is because alkaline and alkaline earth metal catalysts that remained in ash, or were added with the NaOH, were conducive to inhibiting the graphitization of CC and enhancing the quantity of the amorphous carbon structure in CC and ACCs, which corresponds to the report of Wei et al. [27]. Furthermore, it was seen that the peaks of disordered and ordered graphite structures trended to undergo a small shift toward larger angles with increasing NaOH concentration from 0 M to 3 M. This indicated that the stacking thickness of the graphitic layers in ACCs is slightly changing to the thickness of a more amorphous carbon phase [31]. This is attributed to the penetration of H_2O and metal ions into the graphitic layers, causing swelling [18] and the catalytic effect of the metal compounds leading to the cracking of CC and ACCs [27]. At the same time, the compounds K_2O, CaO, Na_2O, K_2CO_3, $CaCO_3$, and Na_2CO_3 [30, 32-35] are also formed during the carbonization and activation stages by redox reactions (Eqs. (6-7)) [23] and carbonate decomposition reaction (Eqs. (8), (10)) [33]. The content of these compounds increases with increasing NaOH concentrations from 0 M to 3 M. This is attributed to more extensive gasification and partial oxidation of the carbon matrix and an increased amount of added Na (Eqs. (9-10)) with increasing NaOH concentrations [23].

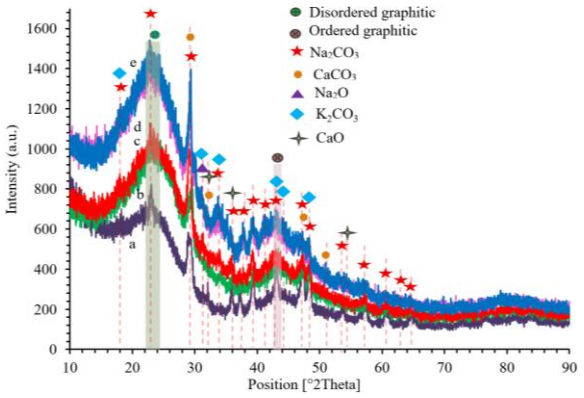

Fig. 3. XRD patterns of a) CC, b) ACC0-600, c) ACC1-600, d) ACC2-600, and e) ACC3-600

3.5. Surface Morphological Characterization of CC and ACCs by FESEM

Surface morphologies of CC showed condensed texture containing a large number of small sized

[DOI: 10.22068/ijmse.4430]

particles adhering on the surface and in the meso-macro hole channel cross section (Fig. 4a).
In addition, there are remaining cell walls on the outer surfaces (Fig. 4b). It was shown that the CC structure was only minimally destroyed during the carbonization stage. After activation with 600 W microwave irradiation in the absence of NaOH (only water), morphologies of ACC0-600 showed a low number of small adhered particles and a rift on the surface (Fig. 4c-d). Furthermore, the wrinkled cell walls of ACC0-600 have disappeared, while some open holes have appeared. This showed that more carbon degradation took place through the action of water molecules (from 0 M NaOH) and metal ions (from the ash content of raw tamarind wood) during microwave activation. Moreover, the surface morphologies of ACCs have become more fractured and increased with increasing NaOH concentration from 1 M to 3 M for both cross-sectional and longitudinal surfaces (Fig. 4e-j). In addition, the number of adhered small particles also increases with increasing NaOH concentration. This is attributed to the small ionic radius and large dipole moment of the Na^+ ion, which could be intercalated in between the layers of charcoal [36], resulting in increased carbon degradation in the CC matrix during microwave activation.

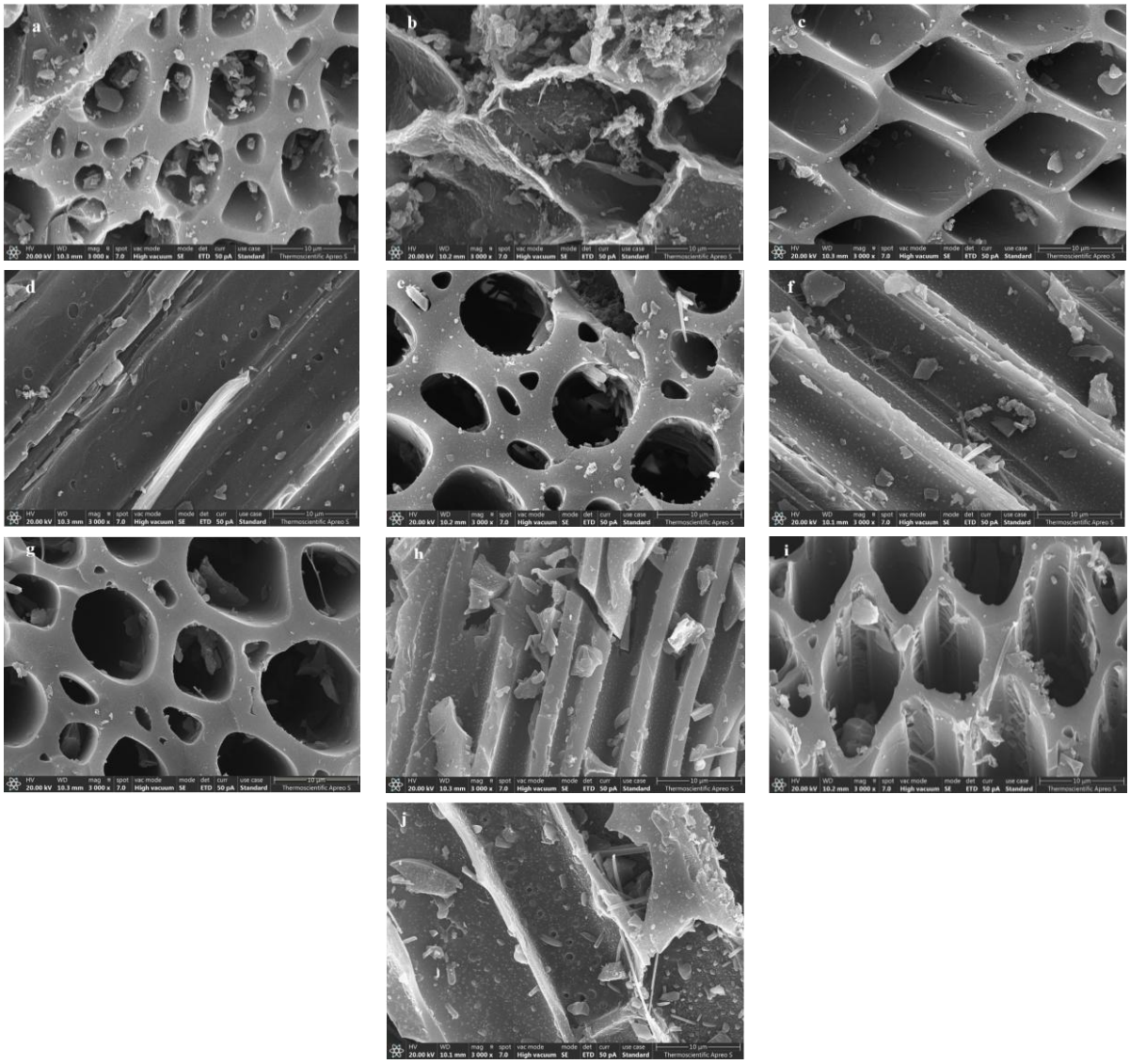

Fig. 4. FESEM morphologies of CC a) cross-sectional and b) longitudinal surface, ACC0-600 c) cross- sectional and d) longitudinal surface, ACC1-600 e) cross-sectional and f) longitudinal surface, ACC2-600 g) cross-sectional and h) longitudinal surface, and ACC3-600 i) cross sectional and j) longitudinal surface

[DOI: 10.22068/ijmse.4430]

However, it was seen that the cross-sectional surface texture (hard core) of ACCs is destroyed to a lesser extent than the longitudinal surface texture (soft core), which corresponds to the report of Koshani et al. [37]. This is attributed to the low intensity of the microwave for the dipole moment of Na^+ ions that pass through the CC surface. Carbon-based materials have high dielectric loss and low magnetic loss characteristics, which improve the absorption of electromagnetic waves, thereby leading to a reduction in penetration depth with decreasing microwave intensity [38]. However, these morphological characteristics (e.g., meso and macro hole channels and fractures) of ACCs are suitable for adsorption or catalytic heterogeneous reactions [39].

3.6. Porosity Characteristics of CC and ACCs

Surface areas of ACCs are increased by about 5-9 times after activation with 0 M–3 M NaOH as compared to CC (Fig. 5A). This is attributed to H_2O, some alkali metals in ash, and NaOH acting as an activating agent by reacting with the carbon material. In addition, microwave heating provides rapid and efficient energy transfer for fast and effective activation. This is consistent with the surface morphological characterization of ACCs from FESEM analysis (Fig. 4). These results have confirmed that the degradation of cell walls and small particles by water and NaOH activation had occurred on the surface of CC with clear open holes and fractures. At the same time, the total pore volumes of ACCs also increased by about 4-6 times from the total pore volume of CC (Fig. 5B-a). Furthermore, the micropore volumes of ACCs are highly increased after activation (Fig. 5B-b). This is the main reason for the significant increase in the surface areas. The average pore diameter values of all ACCs are in the range of 4.24 nm to 12.22 nm, which suggests a mesoporous character; however, the significant increase in micropore volume (Fig. 5B-b) indicates the co-development of microporosity. This is attributed to the energized solvated sodium (size 0.93 nm), which undergoes vigorous motions (e.g., translational motion and rotational motion), which could migrate to or insert into the CC surface and create large pores for producing mesoporous ACCs [20]. This result corresponds to the report of Konno et al. [16], which has pointed out that mesopores are formed more extensively after 3 min of 300 W microwave irradiation. Moreover, these parameter values increased with increasing NaOH concentration from 0 M to 3 M. However, the rates of increase in these values declined with the increase of the concentration of the NaOH activation from 2 M to 3 M NaOH. This indicated that the increase of the NaOH concentration had facilitated the development of new pores or widened the existing pores present on the surface of the ACCs. However, further increases in the NaOH concentration to 3 M had caused a relative increase in the porosity parameters.

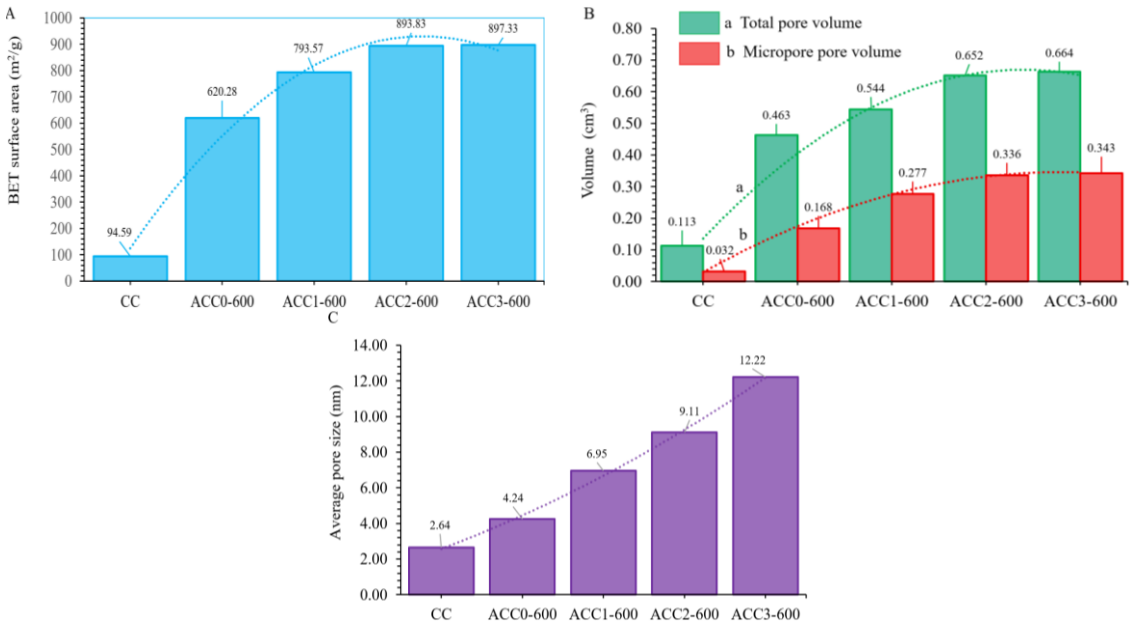

Fig. 5. Plots of BET surface area A), pore volume B-a) and micropore volume B-b), and average pore size C) of CC and ACCs

[DOI: 10.22068/ijmse.4430]

Thus, it can be concluded that the 3 M NaOH concentration was too high and could over-react with the carbon structure resulting in the destruction of the pores. Therefore, 2 M is the optimum NaOH concentration for activation of CC to obtain high-performing ACCs.

3.7. Conversion of Nitrite to Nitrate

The experiments investigating the conversion of nitrite to nitrate were operated with ambient air in the absence of light at pH 6.5, shaking at 120 rpm, and a temperature of 30°C. The absence of light eliminates the possibility of microorganism based nitrification activity so that the results are based only on the process facilitated by ACCs catalytic ability [40]. The slightly acidic conditions of pH 6.5 promote main catalytic oxidation (Eq. (1)) and inhibit the formation of the unwanted secondary pollutant NO through the disproportionation reaction (Eq. (2)) [8]. Shaking of the reaction mixture at 120 rpm ensures a constant supply of dissolved oxygen and good contact between the nitrite ions, dissolved oxygen, and the CC or ACCs particles, which improves mass transfer and reaction rates. Finally, the temperature of 30°C provides an optimal thermal environment for the reactions to proceed, preventing excessively high temperatures that could affect the stability of the CC or ACCs and the kinetics of the reaction. For these reasons, these conditions, except the absence of light, are identical with the natural conditions of environmental air oxidation reaction [41]. Therefore, the catalytic oxidation reaction by catalysts is almost complete, which is desirable for nitrate formation, because nitrates are more stable, less polluting, and could be used as fertilizer for water plants' growth [42].

3.7.1. Effect of dosage and reaction time

ACC2-600 was collected for the study of the effect of dosage on total nitrite conversion. It was shown that the percent of NC_T increased with increasing ACC dosage from 0 g/L to 8 g/L (Fig. 6). This is attributed to the increasing surface area available for the adsorption of oxygen and nitrite with increasing dosage. This phenomenon influences the efficiency of the catalytic oxidation. It was confirmed that the nitrite conversion was catalyzed by ACC. It was also seen that the rates of total nitrite conversion increase significantly in the dosage range from 0.5 g/L to 3 g/L and gradually increase with dosage over 3 g/L. It was shown that further increases in surface for catalytic nitrite oxidation over the dosage of 3 g/L is redundant under these conditions. However, the results achieved with ACC are significantly better than those achieved with zeolite (around 20%-32%) [8] under identical conditions. This may be attributed to the low concentrations of H^+ ion (in the form of H_3O^+ ion) and dissolved oxygen at pH 6.5 and 120 rpm shaking at 30°C with air atmosphere, even though there is remaining nitrite present. Therefore, the 3 g/L dosage was used in further experiments. Furthermore, an insignificant amount of nitrite conversion occurred in the absence of ACC. It was shown that no disproportionation reaction occurred during the air oxidation process. The effect of reaction time on nitrite conversion was investigated as well (Fig. 7).

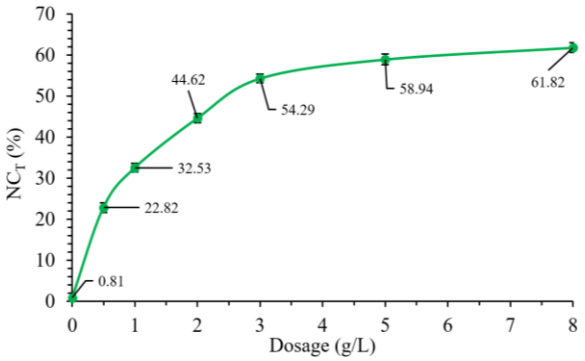

Fig. 6. Percent of total nitrite conversion with dosage (0-8 g/L) of ACC2-600 under conditions: $C_{i\ nitrite}$= 100 mg/L, V= 100 ml, Temperature =30°C, Time= 120 min, and pH= 6.5 (the error bars represent standard deviation)

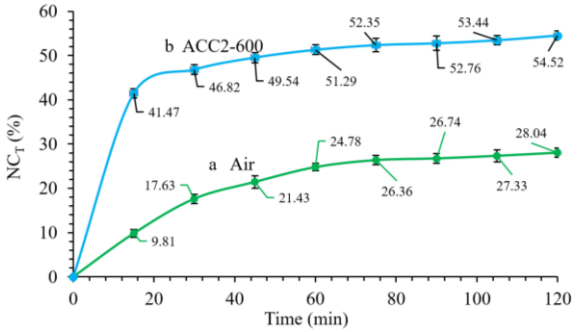

Fig. 7. Percent of total nitrite conversion with reaction time (0-120 min) and dosage (3 g/L) of a) air without ACC, and b) air with ACC2-600, under conditions: $C_{i\ nitrite}$= 100 mg/L, V= 100 mL, T= 30°C, and pH= 6.5 (the error bars represent standard deviation)

The results show that nitrite conversion proceeds with a high reaction rate within the initial 20 min.

[DOI: 10.22068/ijmse.4430]

The reaction rate for reactions with added ACC declined after 30 min, while it gradually increased for air oxidation in the absence of ACC at all time points. This result is consistent with the report of Ying et al. [8]. It was shown that ACC acted as a catalyst for nitrite oxidation conversion with a short reaction time and high percent conversion. The percent of total nitrite conversion in the presence of ACC is higher for the reaction carried out only with air. However, the nitrite conversions in both reactions are continuing with relatively slow reaction rates after 45 min. Therefore, the time point of 60 min was selected for further experiments.

3.7.2. *Effects of NaOH concentration, activation, and recycling*

The effects of carrying out the reaction in air without catalyst, in air with CC, and in air with ACC0-600–ACC3-600 (which are affected by NaOH concentration used for activation), are presented in Fig. 8.

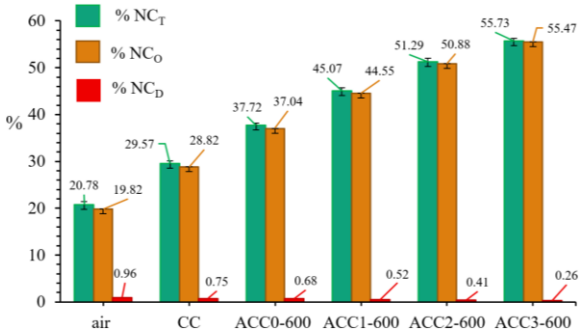

Fig. 8. Conversion of nitrite to nitrate by only air without a catalyst, with CC or ACCs under conditions of $C_{i\ nitrite}$= 100 mg/L, V= 100 mL, T= 30°C, Dosage= 3 g/L (if used), Time= 60 min, and pH= 6.5 (the error bars represent standard deviation)

It was shown that the values of percents of NC_T and NC_O are almost identical and increased after the addition of CC or ACCs in comparison to reactions carried out only with air in the absence of CC or ACCs. It was seen that the oxidation reaction of nitrite being converted into nitrate dominates for reaction conditions of pH 6.5 under an air atmosphere in the absence of light, with and without catalysts. Furthermore, values of percents of NC_T and NC_O increased with the addition of ACC0-600, ACC1-600, ACC2-600, and ACC3-600, respectively, while percentages of NC_D are very low. This indicates that a near-complete selectivity for the oxidative pathway was achieved with ACCs. It was observed that the percentages of NC_O increased dramatically by approximately 9-36% times in comparison with reactions carried out only in air without CC or ACCs, after the addition of CC, ACC1-600, ACC2-600, and ACC3-600, respectively. These results were achieved due to increased surface areas, total pore volume, micropore volume, average pore size, meso and macro hole channels, surface functional, and carbonate observed with increasing NaOH concentration used for ACCs preparations. The reaction mixture can easily enter the meso and macro-sized channels [2] for nitrite ion distribution to adsorption on the surface and micropores of CC or ACCs. At the same time, the amount of adsorbed nitrite increased with increasing surface area, pore volume, micropore volume, and micropore size. Micropore volume and micropore size are especially appropriate for nitrite ion adsorption, because the hydrated diameter of nitrite ion is approximately 1.02 nm, which is less than the micropore size of CC and ACCS (2.64-12.22 nm). In addition, NO_3^- species were generated from –C=C, and –C=O sites on the catalyst's surface [7]. This has confirmed that CC or ACCs acted as catalysts for surface catalysis of nitrite oxidation into nitrate with increasing collision probability and promoting the oxidation of NO_2^- ion to NO_3^- ion [2], while the disproportionation reaction was inhibited. However, the products of the disproportionation reaction are still formed under all experimental conditions. This is attributed to the small concentration of H^+ ions that are present in the weakly acidic (pH 6.5) reaction mixture. However, the percentages of NC_T and NC_O achieved with all investigated catalysts are still low in comparison to the report of Ying et al. [8] and Zhang et al. [2], which were carried out using the strongly oxidizing ozone and strongly acidic (pH 3) conditions. However, this approach exhibits mildness and selectivity. This is attributed to the low oxidizing power of oxygen gas and the weakly acidic (pH 6.5) condition used in this research. Therefore, the current work must be further developed with the use of d-transition element doping into ACC and biological cooperation for reducing reaction time and further accelerating the catalytic oxidation under flowing water and sunlight. This is expected to improve the performance because microorganisms can efficiently utilize oxygen in solutions with pH values within the range between 6.5 and 8.5 [41]. In addition, it

[DOI: 10.22068/ijmse.4430]

could be applied in hydroponic and aquaponic culture for nitrate use and stimulation toward a shifted equilibrium. The effects of air and ACCs catalysts on oxidative nitrite conversion under the conditions used in this research indicated that the oxidation reaction of nitrite by oxygen in air mainly proceeded by adsorption on the surface of CC and ACCs. The adsorption capacity of nitrite ions and oxygen on ACCs increased with increasing NaOH concentration. In addition, the carbonates in CC and ACCs also act as buffers for H^+ ion adsorption, which reduces the disproportionation reactions [43] and aids the adsorption of the negative nitrite ions, resulting in high catalytic oxidation conversion. At the same time, the buffering action of carbonates also results in the loss of Ca, K, and Na [6]. Moreover, the pH 6.5 of the solution is lower than the point of zero charge of these carbonates (> 7) [44]. Therefore, the surfaces of these carbonates consumed protons and attracted NO_2^- ions, which can accelerate the oxidation conversion [6]. Furthermore, surface hydroxyl (OH) species and surface carboxyl groups (COOH) could also improve the conversion rate and oxidation of the adsorbed NO_2^- ion on the ACCs and into NO_3^- ion, and reduce the selectivity of the disproportionation reaction. This is because the oxygen of hydroxide produces hydroxyl radicals from the breakdown of oxygen molecules [2]. Moreover, the negative nitrite ions in solution were drawn closer to the surface of the ACCs by Na^+ ions within the layers of the ACCs. Therefore, the conversion of nitrite ions during the catalytic oxidation on the surface of the ACCs increased with increasing NaOH concentration used for ACCs activation. This is due to the increased content of the oxygenated functional groups (such as –C–O and OH species) as basic adsorption sites [7]. The disproportionation reaction, which releases NO to the gas phase, causing secondary pollution [8], has occurred to a very limited extent due to the very low concentration of free H^+ ions in solution. These results could be summarized in three steps. The first step: nitrite ions from the solution were adsorbed onto the surface of the ACCs. The second step is the catalytic step with ACCs involving a transfer of electrons from the adsorbed nitrite ions to the dissolved oxygen and subsequent nitrate formation. Finally, the nitrate ions are desorbed from the ACC's surface back into the solution.

3.7.3. The reusability of the catalyst

The reusability of the spent catalyst is a key factor to be considered for practical applications [45]. The conversion recycling experiments with CC or ACCs were carried out for up to two recycling repeats of the oxidation of nitrite to nitrate to assess the stability of the catalysts. It was found that a relative decrease in the percentages of NC_T and NC_O for the catalyst used in the first and second recycling runs (Fig. 9) was observed across all catalysts in comparison with the fresh catalyst (Fig. 8). Furthermore, differences in the percentage of NC_T and NC_O of spent catalysts increased with increasing number of recycling steps. This may be due to the erosion and leaching of the catalyst particles over many repeats of the operation. However, the conversion performance tends to be similar to the effects of NaOH concentration during activation. This may be related to the erosion of carbonates and leaching of small particles during the shaking of the reactions and filtration, which is consistent with the hydrodynamic action of carbonate rocks [46] and catalytic oxidation of reactive dye blue 222 by Fe-corn cobs activated carbon catalyst [45]. This is because carbonates are soluble in acidic solutions, and small particles have weak adhesion to solid surfaces [46]. This results in a decrease in the buffering capacity and surface area of the catalysts. Therefore, it may be suggested to increase the reaction time during later recycling or catalyst regenerating experiments. However, it was found that ACC's catalyst demonstrated stable catalytic oxidation activity across three cycles, with oxidation conversion efficiency consistently in the range 32.22%-49.48%, which had decreased by 4.82%-5.99%, while the dis-proportionation reaction was effectively suppressed accounting for only 1.15%-1.49% of the conversion. The cycling stability and structural durability of catalysts are critical metrics for evaluating their industrial applicability, as these properties directly determine process economics and environmental benefits [2]. After two steps of recycling, the contents of some carbonate compounds and C=O are reduced, which is confirmed by the FTIR result (Fig. 10-A), as compared to the original catalyst (only ACC3-600 is shown). This is because carbonates are soluble in acidic solutions [46], while C=O was bonded with hydrogen and transferred to the hydroxyl group of the COOH intermediate, forming water and causing CO_2 to desorb as a molecule [47]. This result has dominated the characteristics of the activated carbon, which exhibits increased intensities of C=C and C-O surface functional groups [48].

[DOI: 10.22068/ijmse.4430]

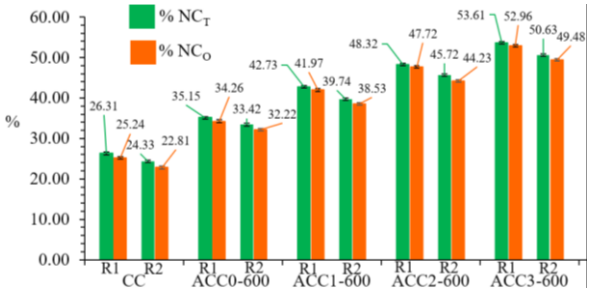

Fig. 9. Percent NC_T and NC_o from a) conversion during first recycling step (R1), and b) conversion during second recycling step (R2) of nitrite oxidation to nitrate by CC or ACCs under conditions of $C_{i\ nitrite}$= 100 mg/L, V= 70 mL for first recycling or 50 mL for second recycling, T= 30°C, Dosage= 3 g/L, Time= 60 min, and pH= 6.5 (the error bars represent standard deviation)

Moreover, the bands of nitrite (1260 to 1300 cm^{-1}) and nitrate (1330 to 1400 cm^{-1}) [49] had not appeared for spent ACC3-600. This indicated that almost all nitrites had been converted into highly soluble free nitrate ions, and then the soluble free nitrate ions and the remaining very mobile nitrite ions were readily leached into the filtrate during filtration [50]. In addition, EDS investigation of spent ACC3-600 after two recycling steps (Fig. 10-B) showed that the contents of O, K, Na, and Ca elements decreased in comparison to the original ACC3-600 (Table 1), while the content of C element increased. This observation was confirmed by the SEM image (Fig. 10-C), which showed some surface erosion and decreased content of small particles in comparison with fresh ACC3-600 (Fig. 4-i). These effects result in decreases in the weights of spent CC and spent ACCs with increasing number of recycling steps (Fig. 10-D). Furthermore, percentages of weight loss increased in the order CC, ACC1-600, ACC2-600, and ACC3-600, respectively, for all recycling experiments, which is in line with the effects of NaOH concentration during activation. It was shown that carbonate compounds and small particles in the catalysts were eroded during the conversion reactions and filtering. Since the degree of activation increases with increasing NaOH concentration, more carbonates and smaller particles are formed, resulting in a higher percentage weight loss in spent catalysts, which is consistent with the report of Ao et al. [51]. Nevertheless, some carbonates and small particles remained on the spent catalyst because the reaction occurred under weakly acidic conditions and with gentle shaking. Besides, lowering percents of weight loss were observed for all catalysts with increasing conversion recycling time. This is because a large number of carbonates and small particles have been eroded and leached in the first steps of the conversions [52].

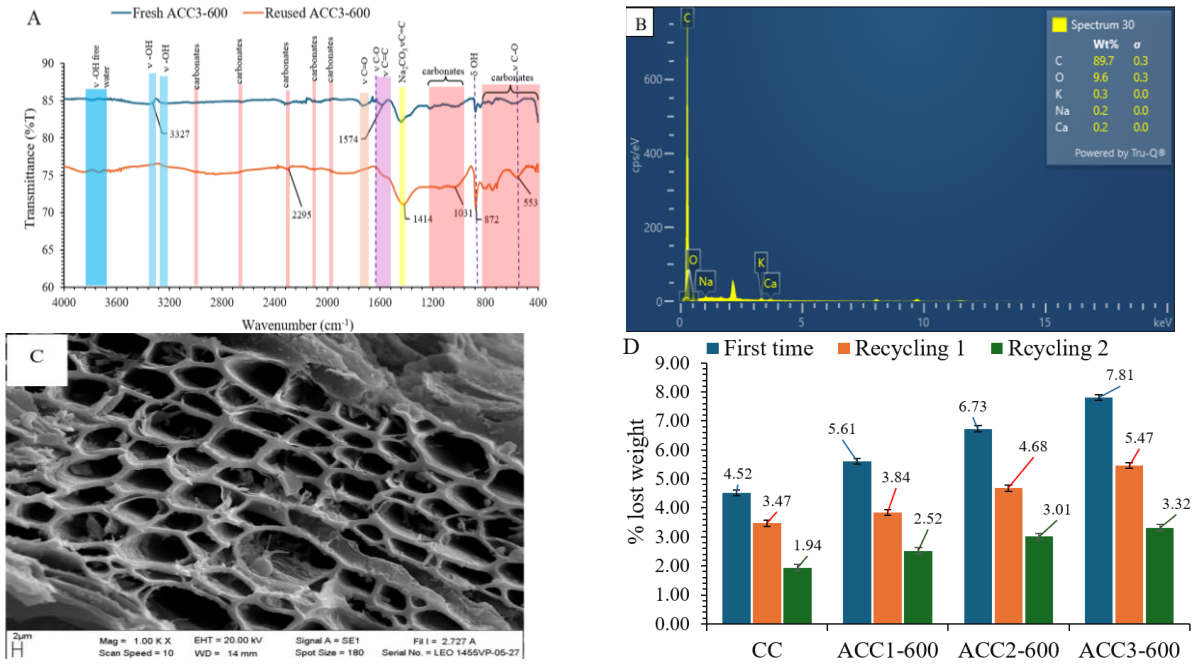

Fig. 10. A) FTIR transmission spectra of fresh ACC3-600 and reused ACC3-600 after recycling two times, B) EDS of reused ACC3-600 after recycling two times, C) SEM of reused ACC3-600 after recycling two times, D) percent weight loss of CC and ACCs after oxidation conversion at first time, first recycling, and second recycling (the error bars represent standard deviation)

[DOI: 10.22068/ijmse.4430]

4. CONCLUSIONS

The preparations of ACCs were investigated by exploring the effects of NaOH concentration with ratios of CC weight to NaOH weight of 1 g: 0 g, 1 g: 0.04 g, 1 g: 0.08 g, and 1 g: 0.12 g (pretreatment by boiling 0-3 M NaOH solution) and 600 W microwave irradiation activation. It was seen that the percent yields of ACCs gradually decreased with increasing NaOH concentration from 0 M to 3 M, which have values in the range between 35.65% and 38.13% based on tamarind wood weight calculation or 88.51 and 94.66% based on CC weight calculation. The elemental composition of CC and ACCs includes carbon, oxygen, and small amounts of Ca, Na, and K. In addition, it was found that the main carbonate surface functional group of ACCs is present after partial oxidation. At the same time, the contents of amorphous carbon allotropes of ACCs are increased with increasing NaOH concentrations. The swelling of graphitic layers has taken place during the pretreatment by boiling in NaOH solution. The Na^+ ions and water molecules could be inserted into the graphitic layers and rapidly induce surface cracking of ACCs by 600 W microwave irradiation. The extent of surface cracking of ACCs increased with increasing NaOH concentration from 1 M to 3 M for both cross-sectional and longitudinal surfaces. These phenomena have resulted in an increase in the porosity of ACCs with average mesopore size in the range from 4.24 nm to 12.22 nm. Furthermore, meso and macro-sized hole channels were also presented within the ACCs. These characteristics are suitable for adsorption or catalytic heterogeneous reactions. However, the optimum concentration for the activation of CC to obtain high-performance ACCs is 2 M NaOH or 1 g CC: 0.08 g NaOH. Subsequently, the conversions of nitrite into nitrate were affected by CC or ACCs catalysts under an air atmosphere in the absence of light, at 30°C, pH 6.5, and 120 rpm shaking. It was found that the nitrite conversions are rapid within 20 min of ACC addition, while they gradually increased in speed for air oxidation without ACC at all times. It was shown that ACC acted as a catalyst for nitrite oxidation conversion with a short reaction time and a high percent conversion. Moreover, the values of percents of NC_T and NC_O increased with adding ACC0-600, ACC1-600, ACC2-600, and ACC3-600, respectively, achieving conversion 9-36% times higher in comparison to operations carried out without CC or ACCs, while NC_D was inhibited. It was shown that ACC significantly enhances the oxidation rate. The great extent of nitrite conversions by catalytic oxidation was ascribed to the high content of surface areas, total pore volume, micropore volume, average pore size, meso and macro hole channels, and carbonate on ACCs products, which could be adapted for natural environment wastewater treatments with decreased operational costs. In addition, spent ACCs can be used for oxidation conversion recycling with 4.82%-5.99% NC_O efficiency reduction after three recycling steps. However, it was seen that nitrite ions in filtered solutions remain present under these conditions. Therefore, this operation must be further developed by improving ACC with d-transition element doping and/or biological cooperation for reducing reaction time and increasing the acceleration of catalytic oxidation under flowing water and sunlight.

ACKNOWLEDGEMENT

The authors would like to thank the Chemistry Department and Science Laboratory Center, Faculty of Science, Naresuan University, for all their support.

DECLARATION OF GENERATIVE AI AND AI-ASSISTED TECHNOLOGIES

The data and writing process do not pertain to the use of AI tools for data analysis or drawing insights as part of the research itself.

REFERENCES

[1] Boasiako, C.A., Zhou, Z., Huo, X., Ye, T., "Development of Pd-based catalysts for hydrogenation of nitrite and nitrate in water: A review", J. Hazard. Mater. 2023, 446, 130661. doi: 10.1016/j.jhazmat.2022.130661.

[2] Zhang, Y., Sun, Y., Zhu, Y., Weng, W., He, Y., Wang, Z., "Catalytic ozonation of nitrite in denitrification wastewater based on Mn/ZSM-5 zeolites: Catalytic performance and mechanism", Processes 2025, 13, 2387. doi: 10.3390/pr13082387.

[3] Wang, Y., Li, B., Li, G., Huang, Y., Fang, D., Wang, J., Song, Y., "Photocatalytic conversion of nitrite in aqueous solution over nanocomposite photocatalyst Er^{3+}: $Y_3Al_5O_{12}/BiPO_4$ using different photosources",

[DOI: 10.22068/ijmse.4430]

J. Ind. Eng. Chem. 2017, 47, 74-85. doi: 10.1016/j.jiec.2016.11.016.

[4] Guan, B., Chen, J., Zhuang, Z., Zhu, L., Ma, Z., Hu, X., Zhu, C., Zhao, S., Shu, K., Dang, H., Gao, J., Zhang, L., Zhu, T., Huang, Z., "Study on the effect and mechanism of Fe doping on $Fe_{0.2}Ce_{0.8}O_2$-δ CDPF catalyst for NOx-assisted soot catalytic oxidation", Mater. Chem. Phys. 2025, 338, 30636. doi: 10.1016/j.matchemphys.2025.130636.

[5] Date, M., Jaspal, D., "Catalytic degradation of ammonia and nitrate from wastewater-A critical review", Adv. Environ. Technol. 2022, 3, 239-253. Doi: 10.22104/AET.2022.5764.1580.

[6] Velázquez-Palenzuela, A., Ulusoy, B., Dam-Johansen, K., Christensen, J. M., "Photo-oxidation of nitrite anions in aqueous solution for the benchmarking of nano-TiO_2 photocatalytic coatings", Prog. Org. Coat. 2023, 175, 107380. doi: 10.1016/j.porgcoat.2022.107380.

[7] Liu, Y., Gao, F., Yi, H., Yang, C., Zhang, R., Zhou., Y., Tang, X., "Recent advances in selective catalytic oxidation of nitric oxide (NO-SCO) in emissions with excess oxygen: a review on catalysts and mechanisms", Environ. Sci. Pollut. Res. 2012, 28, 2549–2571. doi: 10.1007/s11356-020-11253-6.

[8] Ying, M., Zhang, M., Liu, Y. Wu, Z., "Ozone-assisted catalytic oxidation of aqueous nitrite ions on HZSM-5 zeolites", Sci. Rep. 2019, 9, 14322. doi: 10.1038/s41598-019-50662-7.

[9] Yin, C., Li, Y., Zhang, T., Liu, J., Yuan, Y., Huang, M., "Effects of exposure to anionic surfactants (SDBS and SDS) on nitrogen removal of aerobic denitrifier", Water. Environ. Res. 2020, 92(2), 2129-2139. doi: 10.1002/wer.1384.

[10] Shih, Y. J., Lin, P. Y., Wu, Z. L., "Catalytic oxidation and deionization of nitrite and nitrate ions using mesoporous carbon-supported nano-flaky cobalt and nickel oxyhydroxides", J. Colloid Interface Sci., 2022, 611, 265-277. doi: 10.1016/j.jcis.2021.12.085.

[11] Takayanagi, T., Kimiya, H., Ohyama, T., "Formation of artifactual DMPO-OH spin adduct in acid solutions containing nitrite ions", Free Radic. Res. 2017, 51(7–8), 739–748. doi: 10.1080/10715762.2017.1369536.

[12] Ernst, A., Steinbach, C., Wagner, K., Waller, U., "Virtual sensing of nitrite: A novel control for safe denitrification in recirculating aquaculture systems (RASs)", Fishes 2024, 9, 398. doi: 10.3390/fishes9100398.

[13] Urbina-Suarez, N. A., Barajas-Solano, A. F., Zuorro, A., Machuca, F., "Advanced oxidation processes with uv-H_2O_2 for nitrification and decolorization of dyehouse wastewater", Chem. Eng. Trans. 2022, 95, 235-240. doi: 10.3303/CET2295040.

[14] Pallarés, J., González-Cencerrado, A., Arauzo, I., "Production and characterization of activated carbon from barley straw by physical activation with carbon dioxide and steam", Biomass Bioenergy 2018, 115, 64-73. doi: 10.1016/j.biombioe.2018.04.015.

[15] Mistar, E. M., Ahmad, S., Muslim, A., Alfatah, T., Supardan, M. D., "Preparation and characterization of a high surface area of activated carbon from Bambusa vulgaris —Effect of NaOH activation and pyrolysis temperature", IOP Conf. Ser.: Mater. Sci. Eng. 2018, 334, 012051. doi: 10.1088/1757-899X/334/1/012051.

[16] Konno, K., Oike, Y., Ohba, Y., Sasaki, O., Takiguchi, Y., Onoe, K., Yamaguchi, T., "Short-time preparation of NaOH-activated carbon from sugar cane bagasse using microwave plasma heating", Green Sustain. Chem. 2017, 7, 259-269. doi: 10.4236/gsc.2017.74020.

[17] Cai, C., Ge, T., Zhang, M., Zhao, Y., Wu, C., Han, J., "Effect on combustion properties of coal treated by microwave irradiation combined with sodium hydroxide solution", Processes 2021, 9, 1284. doi: 10.3390/pr9081284.

[18] Bala, R., Mondal, M. K., "Exhaustive characterization on chemical and thermal treatment of sawdust for improved biogas production", Biomass Convers. Biorefin. 2018, 8, 991-1003. doi: 10.1007/s13399-018-0342-6.

[19] Foo, K. Y., Hameed, B. H., "Microwave-assisted preparation and adsorption performance of activated carbon from biodiesel industry solid residue: Influence of operational parameters", Bioresour. Technol. 2012, 103(1), 398-404. doi: 10.1016/j.biortech.2011.09.116.

[20] Liew, R. K., Azwar, E., Yek, P. N. Y., Lim,

[DOI: 10.22068/ijmse.4430]

X. Y., Cheng, C. K., Ng, J. H., Jusoh, A., Lam, W. H., Ibrahim, M. D., Ma, N. L., Lam, S. S., "Microwave pyrolysis with KOH/NaOH mixture activation: A new approach to produce micro-mesoporous activated carbon for textile dye adsorption", Bioresour. Technol. 2018, 266, 1-10. doi: 10.1016/j.biortech.2018.06.051.

[21] Sreekumar, N. V., Narayana, B., Hegde, P., Manjunatha, B. R., Sarojini, B. K., "Determination of nitrite by simple diazotization method", Microchem. J. 2003, 74(1), 27-32. doi: 10.1016/S0026-265X (02)00093-0.

[22] Jaworski, M. A., Siri, G. L., Casella, M. L., "A simple and sensitive spectrophotometric determination of nitrate and nitrite in water samples", Asian J. Research Chem. 2011, 4(11), 1655-1660.

[23] Aloud, S. S., Alharbi, H. A., Hameed, B. H., Giesy, J. P., Almady, S. S., Alotaibi, K. D., "Production of activated carbon from date palm stones by hydrothermal carbonization and microwave-assisted KOH/NaOH mixture activation for dye adsorption", Sci. Rep. 2023, 13, 19064. doi: 10.1038/s41598-023-45864-z.

[24] Damion Williams, W., Greeley, J. P., Delgass, W. N., Ribeiro, F. H., "Water activation and carbon monoxide coverage effects on maximum rates for low temperature water-gas shift catalysis", J. Catal. 2017, 347, 197-204. doi: 10.1016/j.jcat.2017.01.016.

[25] Sahu, J. N., Acharya, J., Meikap, B. C., "Optimization of production conditions for activated carbons from Tamarind wood by zinc chloride using response surface methodology", Bioresour. Technol. 2010, 101(6), 1974-1982. doi: 10.1016/j.biortech. 2009.10.031.

[26] Bouchelta, C., Chekkat, F. A., Marsa, Z., Ramdane, N., Mechatti, F., Medjram, M. S., "Preparation of activated carbon from a petrochemical industrial waste by NaOH activation under microwave radiation, application in dyes adsorption", Jordan J. Chem. 2021, 7(3), 253-266.

[27] Wei, X. N., Li. T. T., "Wooden activated carbon production for dioxin removal via a two-step process of carbonization coupled with steam activation from biomass wastes", ACS Omega. 2021, 6(8), 5607-5618. doi: 10.1021/acsomega.0c06032.

[28] Sung, W., Inoue, K., Nihonyanagi, S., Tahara, T., "Unified picture of vibrational relaxation of OH stretch at the air/water interface", Nat. Commun. 2024, 15, 1258. doi: 10.1038/s41467-024-45388-8.

[29] Ibrahim, S., Ahmad, A., Mohamed, N. S., "Characterization of novel castor oil-based polyurethane polymer electrolytes", Polymers. 2015, 7, 747-759. doi: 10.3390/polym704 0747.

[30] Bahranowski, K., Klimek, A., Gaweł, A., Serwicka, E. M., "Rehydration driven Na-activation of bentonite—evolution of the clay structure and composition", Materials. 2012, 14, 7622. doi: 10.3390/ma14247622.

[31] Keppetipola, N. M., Dissanayake, M., Dissanayake, P., Karunarathne, Dourges, M. A., Talaga, D., Servant, L., Olivier, C., Toupance, B. T., Uchida, S., Tennakone, K., Kumara, G. R. A., Cojocaru, L., "Graphite-type activated carbon from coconut shell: a natural source for eco-friendly non-volatile storage devices", RSC Adv., 2021, 11, 2854. doi: 10.1039/d0ra09182k.

[32] Febrida, R., Setianto, S., Herda, E., Cahyanto, A., Joni, I. M., "Structure and phase analysis of calcium carbonate powder prepared by a simple solution method", Heliyon. 2021, 7(11), e08344. doi: 10.1016/j.heliyon.2021. e08344.

[33] Kumar, R., Miyaoka, H., Shinzato, K., Ichikawa, T., "Analysis of sodium generation by sodium oxide decomposition on corrosion resistance materials: a new approach towards sodium redox water splitting cycle", RSC Adv. 2021, 11, 21017. doi: 10.1039/d1ra02 671b.

[34] Shkatulov, A. I., Houben, J., Fischer, H., Huinink, H. P., "Stabilization of K_2CO_3 in vermiculite for thermochemical energy storage", Renewable Energy. 2020, 150, 990-1000. doi: 10.1016/j.renene.2019.11.119.

[35] Huh, J. H., Choi, Y. H., Ramakrishna, C., Cheong, S. H., Ahn, J. W., "Use of calcined oyster shell powders as CO_2 adsorbents in algae-containing water", J. Korean Ceram. Soc. 2016, 53(4), 429-434. doi: 10.4191/ kcers.2016.53.4.429.

[36] Dobele, G., Volperts, A., Plavniece, A., Zhurinsh, A., Upskuviene, D., Balciunaite, A., Niaura, G., Colmenares-Rausseo, L. C.,

[DOI: 10.22068/ijmse.4430]

Tamasauskaite-Tamasiunaite, L., Norkus, E., "Thermochemical activation of wood with NaOH, KOH and H_3PO_4 for the synthesis of nitrogen-doped nanoporous carbon for oxygen reduction reaction", Molecules. 2024, 29, 2238. doi: 10.3390/ molecules29102238.

[37] Koshani, R., Pitcher, M. L., Yu, J., Mahajan, C. L., Kim, S. H., Sheikhi, A., "Plant cell wall-like soft materials: Micro- and nanoengineering, properties, and applications", Nanomicro Lett. 2025, 17, 103. doi: 10.1007/s40820-024-01569-0.

[38] Li, Z., Peng, K., Ji, N., Zhang, W., Tian, W., Gao, Z., "Advanced mechanisms and applications of microwave-assisted synthesis of carbon-based materials: a brief review", Nanoscale Adv. 2024, 7, 419-432. doi: 10.1039/d4na00701h.

[39] Manzoor, S., Wani, O. B., Bobicki, E. R., "Investigating the microwave properties of carbon materials from microwave-driven methane pyrolysis", Carbon Trends. 2024, 14, 100326. doi: 10.1016/j.cartre.2024.100326.

[40] Kumar, A., Ng, D. H. P., Bairoliya, S., Cao, B., "The dark side of microbial processes: Accumulation of nitrate during storage of surface water in the dark and the underlying mechanism", Microbiol. Spectr. 2022, 10(1), e0223221. doi: 10.1128/spectrum.02232-21.

[41] Kokina, K., Mezule, L., Gruskevica, K., Neilands, R., Golovko, K., Juhna, T., "Impact of rapid pH changes on activated sludge process", Appl. Sci. 2022, 12, 5754. doi: 10.3390/ app12115754.

[42] Bijay-Singh, Craswell, E., "Fertilizers and nitrate pollution of surface and ground water: an increasingly pervasive global problem", SN Appl. Sci. 2021, 3, 518. doi: 10.1007/s42452-021-04521-8.

[43] Rayaroth, M. P., Aravindakumar, C. T., Shah, N. S., Boczkaj, G., "Advanced oxidation processes (AOPs) based wastewater treatment-unexpected nitration side reactions- a serious environmental issue: A review", Chem. Eng. J. 2022, 430(4), 133002. doi: 10.1016/ j.cej.2021.133002.

[44] Derkani, M. H., Fletcher, A. J., Fedorov, M., Abdallah, W., Sauerer, B., Anderson, J., Zhang, Z. J., "Mechanisms of surface charge modification of carbonates in aqueous electrolyte solutions", Colloids Interfaces. 2019, 3, 62. doi:10.3390/colloids3040062.

[45] Mahanna, H., El-Bendary, N., "Enhanced catalytic oxidation of reactive dyes by reuse of adsorption residuals as a heterogeneous catalyst with persulfate/UV process", Int. J. Environ. Sci. Technol. 2022, 19, 10945-10956. doi: 10.1007/s13762-021-03856-4.

[46] Zhang, J., Chu, X., Fu, H., Zhang, Q., Zong, S., "Investigating the acid erosion characteristics of carbonate rocks under hydrodynamic action", ACS Omega. 2024, 9(17), 18922-18931. doi: 10.1021/acsomega. 3c08557.

[47] Cui, C., Han, J., Zhu, X., Liu, X., Wang, H., Mei, D., Ge, Q., "Promotional effect of surface hydroxyls on electrochemical reduction of CO_2 over SnO_x/Sn electrode", J. Catal. 2016, 343, 257-265. doi: 10.1016/j.jcat. 2015.12.001.

[48] Zheng, J., Xing, X., Pang, Z., Wang, S., Du, Y., Lv, M., "Effect of Na_2CO_3, HF, and CO_2 treatment on the regeneration of exhausted activated carbon used in sintering flue gas", ACS Omega. 2021, 6(39), 25762-25771. doi: 10.1021/acsomega.1c04182.

[49] Bose, S., Bahadorikhalili, S., Yuanyi He, Y., Samouei, H., Zare, R. N., "Highly efficient production of nitrite and nitrate from air at the gas-water interface of nanobubbles", Sci. Adv. 2026, 12, eaec4225. doi: 10.1126/ sciadv.aec4225.

[50] Mohammed, K. A., Umer, M. I., Alyazichi, Y. M., "Biological nitrogen transformation efficiency in removing nitrogen and improving water quality from Zakho municipal wastewater in Kurdistan region/ Iraq", IOP Conf. Ser.: Earth Environ. Sci. 2022, 1120, 012036. doi: 10.1088/1755-1315/1120/1/012036.

[51] Ao, S., Changmai, B., Vanlalveni, C., Chhandama, M. V. L., Wheatley, A. E. H., Rokhum, S. L., "Biomass waste-derived catalysts for biodiesel production: Recent advances and key challenges", Renew. Energy. 2024, 233, 120031. doi: 10.1016/ j.renene.2024.120031.

[52] Xu, K., Huang, M., Liu, Z., Cui, M., Li, S., "Mechanical properties and disintegration behavior of EICP-reinforced sea sand subjected to drying-wetting cycles", Biogeotechnics. 2023, 1(2), 100019. doi: 10.1016/j.bgtech. 2023.100019.

[DOI: 10.22068/ijmse.4430]